Received: 2 December 2020 | Revised: 18 January 2021 | Accepted: 19 January 2021

DOI: 10.1002/jbio.202000477

FULL ARTICLE

JOURNAL OF BIOPHOTONICS

Exploring a possibility of using Raman spectroscopy for detection of Lyme disease

Charles Farber[1] | Rohini Morey[1] | Mark Krimmer[1] | Dmitry Kurouski[1*] | Artem S. Rogovskyy[2*]

[1]Department of Biochemistry and Biophysics, Texas A&M University, College Station, Texas, USA

[2]Department of Veterinary Pathobiology, College of Veterinary Medicine and Biomedical Sciences, Texas A&M University, College Station, Texas, USA

***Correspondence**
Dmitry Kurouski, Department of Biochemistry and Biophysics, Texas A&M University, College Station, Texas, 77843, USA.
Email: dkurouski@tamu.edu
Artem Rogovskyy, Department of Veterinary Pathobiology, College of Veterinary Medicine and Biomedical Sciences, Texas A&M University, College Station, Texas, 77843, USA.
Email: arogovskyy@tamu.edu

Abstract

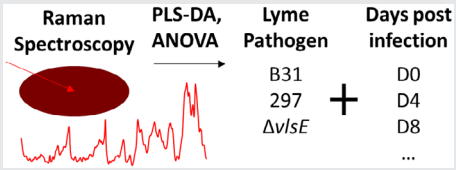

Lyme disease (LD), one of the most prevalent tick-borne diseases in the United States (US), is caused by *Borreliella burgdorferi sensu stricto* (*Bb*). To date, in the US, LD diagnostics is primarily based on validated two-tiered serological testing, which overall exhibits low sensitivity among other drawbacks. In the present study, a potential of Raman spectroscopy (RS) to detect *Bb* infection in mice has been explored. For that, C3H mice were infected with wild-type *Bb* strains, 297, B31, or B31-derived mutant, Δ*vlsE*. Blood samples taken prior to and post *Bb* infection were subjected to RS. The data demonstrated that RS did not directly detect *Bb* spirochetes in blood, but rather sensed biochemical changes associated with *Bb* infection. Despite *Bb* infection-associated blood changes detectable by RS were very limited, the partial least square discriminant analysis showed that the average true positive rates were 86% for 297 and 89% for B31 and Δ*vlsE*.

KEYWORDS

Borrelia burgdorferi, Lyme borreliosis, Raman spectroscopy, blood, specimens, diagnostic test

1 | INTRODUCTION

Lyme disease (LD) is the most prevalent tick-borne illness in the United States (US). Numerous strains of *Borreliella burgdorferi sensu stricto* (*Bb*) are responsible for this debilitating illness in the US.[1] LD is a multisystemic disease with transient flu-like symptoms during its early stage. When this early stage is overlooked, LD patients develop a chronic disease, which is characterized by a variety of severe clinical signs (e.g., arthritis, carditis, peripheral neuropathy, and meningitis).[2] Antimicrobial treatment of chronic LD can be a real challenge. *Bb* may persist for many years[3–8] despite a strong anti-*Bb* immune response.[9–12] Since there is no LD vaccine for humans,[13–18] an effective treatment largely depends on timely diagnosis.

To date, in the US, the only validated approach for LD diagnosis is two-tiered serology.[19, 20] This assay consists of an enzyme immunoassay (EIA) to detect IgM or IgG anti-*Bb* serum antibodies, and western blot (WB), which is only followed when a sample is positive or equivocal by EIA. IgM testing is only recommended over the first 30 days of LD, after which IgG tests (EIA and WB) should be used.[21] Unfortunately, the two-tiered serology has a number of drawbacks, including background seropositivity, cross-reactivity with non-*Bb* antigens, and low sensitivity.[18,22–25] A recent study also showed low diagnostic concordance between laboratories

when different serological assays were used.[25] Lastly, the serological assay cannot distinguish between active or past *Bb* infection or reinfection, the caveat that requires a reliable direct test to be developed.[26]

The LD pathogen, its DNA or proteins can be directly detected in biopsies of skin lesions termed erythema migrans before anti-*Bb* antibodies are developed. To date, however, none of the existing direct methods are more reliable than the two-tiered serological system. Culture is impractical for routine clinical use as it requires specialized media and *Bb* is a slow grower.[27] Antigen-capture assays have low sensitivity and poor specificity.[28] Similarly, the sensitivity of PCR performed on most of patients' tissues, especially blood and cerebrospinal fluid, is very low.[29–33] Together, there is clearly an urgent need in development of reliable direct-detection method, whose overall performance should surpass that of the existing serological assay.

Raman spectroscopy (RS) is a powerful analytical tool designed to detect subtle molecular vibrations of analyzed samples, which often results in their identification.[34] RS is based on the phenomenon of inelastic light scattering by molecules excited to higher vibrational or rotational states. The RS application in the field of disease diagnostics is a rapidly developing field.[35] For instance, Dionne's group demonstrated that 30 different bacterial pathogens can be identified with 97% accuracy by a combination of RS and deep learning approaches.[36] Several research groups have demonstrated that RS could be applied to detect diseases via spectroscopic analysis of body fluids. For example, Ryzhikova and coworkers were able to detect metabolic changes in blood, which were associated with Alzheimer's disease (AD).[37] RS was demonstrated to be pathology-specific and had the capacity to differentiate between AD and other forms of dementia with high accuracy. Moreover, Hobro and colleagues found that Raman-based analysis of metabolic changes in patients' blood could be used to diagnose and also monitor progression of malaria.[38] Lastly, Khan and coworkers showed that viral diseases could also be detected via spectroscopic analysis of blood.[39]

Recently, by using liquid chromatography coupled to mass spectrometry (LC–MS), Molins and co-workers revealed metabolic changes in blood of patients, who had early LD.[40] Specifically, the levels of 62 and 33 molecular species significantly increased and decreased, respectively, in blood of the LD patients compared to healthy individuals (controls). A large number of those molecular species were lipids or their derivatives, including cholesterol, cholesteryl acetate, phospholipids, sphingolipids, diacylglycerol, and triglycerides.[40] Concentration changes were also noted for short peptides and other low-molecular weight species (e.g., 4,8-dimethylnonanoyl carnitine and trans-2,3,4-trimethoxycinnamate). Based on the above, it is possible that some metabolic/biochemical changes associated with LD could be detected by RS. Therefore, the objective of this study was to examine the capacity of RS to detect *Bb* infection.

2 | MATERIALS AND METHODS

2.1 | Ethics statement

The mouse experimental procedures were approved by the Institutional Animal Care and Use Committee of Texas A&M University and performed in accordance with Public Health Service (PHS) Policy on Humane Care and Use of Laboratory Animals (2002), Guide for the Care and Use of Agricultural Animals in Research and Teaching (2010), and Guide for the Care and Use of Laboratory Animals (2011).

2.2 | Bacteria and culture conditions

Fully infectious wild-type *Bb* strains, B31-A3 (B31)[41] and 297,[42] were kind gifts from Patti Rosa and Scott Samuels by way of Troy Bankhead. The B31-A3 lp28-1Δ*vls* (Δ*vlsE*) mutant[43] was kindly provided by Troy Bankhead. Spirochetes were cultivated in liquid Barbour–Stoenner–Kelly II medium supplemented with 6% rabbit serum (BSK-II; Gemini Bio-Products, CA, US) and incubated at 35°C under 2.5% CO_2. For animal tissue culture, BSK-II was supplemented with 0.02 mg ml^{-1} phosphomycin, 0.05 mg ml^{-1} rifampicin and 2.5 mg ml^{-1} amphotericin B to prevent bacterial and fungal contamination.

2.3 | Murine infection and blood sampling

A total of 15 male C3H/HeJ (C3H) mice of 4–6 weeks of age were obtained from the Jackson Laboratories (ME, US). The mice were randomly split into three groups (five animals per group) and, after a short adaption period, the mice of groups A, B, and C were needle inoculated with 1.1×10^4 cells of 297, B31, and Δ*vlsE* per animal, respectively, as described.[44] C3H mice were chosen because these immunocompetent animals develop *Bb*-induced arthritis.[45] The B31 (and its isogenic mutant, Δ*vlsE*) and 297 strains represent two out of the three major *Bb* classes, RST1 and RST2, respectively, which are encountered in the US at a frequency of approximately a third of *Bb* population.[46,47] Each infection was verified by culturing 50 μl of blood harvested at day 7 postinfection (pi) via

maxillary bleed, and other tissues sampled at days 28 pi (ear pinnae) and 56 pi (bladder, ear pinnae, heart, and tibiotarsal joints) as detailed.[48] The presence of *Bb* spirochetes in cultures was confirmed by dark-field microscopy. At days 0, 3, 7, and weekly onwards until day 56 pi, 50 µl of blood was collected from each animal via cheek bleed. Individual blood samples were placed in sterile Eppendorf tubes, which were then stored at −80°C until RS analysis.

2.4 | Raman spectroscopy

Fifty microliters of blood was applied to a foil-wrapped microscope slide by spreading it over as a thin layer. Samples were dried under a fume hood for 1 h. Raman spectra were acquired utilizing a home-built confocal Raman microscope equipped with 785 nm continuous wave laser (Necsel, NJ). By using a set of mirrors, the laser light was brought to the inverted microscope (Nikon TE-2000 U), passed through a 50/50 beam splitter, and focused on the surface of dry blood via 20X Nikon objective (NA = 0.45). Laser power at the objective was ~5.7 mW. The scattered light was directed to an IsoPlane SCT 320 spectrograph (Princeton Instruments, NJ, US), which was equipped with a 600 groove/mm grating blazed at 750 nm. Prior to entering the spectrograph, Rayleigh scattering was filtered with a LP02-785RE-25 long-pass filter (Semrock, NY). The spectrograph-dispersed light was sent to PIXIS:400BR CCD (Princeton Instruments). A motorized stage H117P2TE (Prior, MA) controlled by Prior Proscan II was used to move the sample relative to the incident laser beam. The acquisition time was 10 s per spectrum. Approximately 50 spectra were acquired per *Bb* strain/mutant from spatially non-overlapping locations on the foil per time point and replicate combination. A total of 5813 spectra were acquired and analyzed in the present study.

2.5 | Statistical analysis

All statistical analysis was performed using MATLAB (ANOVA) or MATLAB addon PLS_Toolbox (for PLS-DA, Eigenvector Research, Inc., WA). All spectra were first baseline corrected via the Automatic Weighted Least Squares algorithm with a 6th order polynomial and then

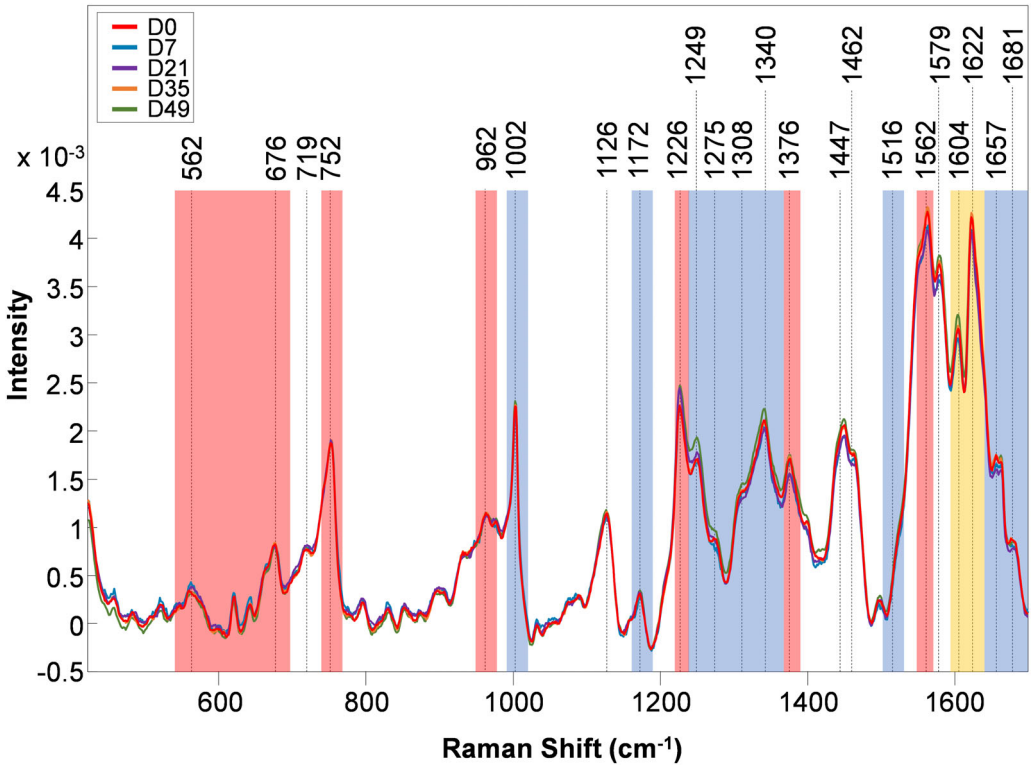

FIGURE 1 Averaged Raman spectra of blood samples taken from *B. burgdorferi* B31-infected C3H mice at selected time points postinfection. Vibrational bands highlighted by red, blue, and yellow can be assigned to heme, protein, and aromatic vibrations, respectively. The other versions of this figure with all the time points for each *Bb* strain/mutant can be found in Figures S9-S11. Vibrational band assignments for Raman spectra of mouse blood are listed in Table 1. D0, D7, D21, D35, and D49 denote, respectively, days 0, 7, 21, 35, and 49 postinfection

normalized to the total spectral area. Analysis of Variance (ANOVA) was conducted by utilizing the preprocessed intensity values at the indicated Raman shifts. All the reported differences were considered significant at the 0.05 level. Post-hoc testing was performed by using the Tukey HSD test, which was utilized to generate the 95% confidence intervals, Figures S1-S8. Prior to the multivariate statistical analysis, spectra were processed with previously described treatments and mean centered.

Partial least squares discriminant analysis (PLS-DA) was used to differentiate mouse blood samples between *Bb* strains/mutant and between different time points. As a result, PLS-DA models were constructed for each time point pairing, which resulted in a total of 45 binary models per *Bb* strain/mutant. To differentiate between *Bb* strains/mutant, the data were averaged by sets of 5 based on the typical averaging size for the binary models. However, the results showed that the signal-to-noise ratio of acquired spectra was insufficient to achieve reasonable accuracy in the built models. The ratio was therefore improved at the cost of sample size by implementing a rolling average scheme. Raw spectra were averaged together in sets of 1 (no averaging) to 6 spectra per mean. These averaged spectra were then used to construct new models. The best performing model (the highest true positive rate [TPR] and Matthews correlation coefficient [MCC]) was retained and reported.

3 | RESULTS

In this preliminary, proof-of-concept study, the potential of RS utility for the diagnosis of LD has been investigated. For that, C3H mice were infected with 297, B31, or B31-derived isogenic mutant, Δ*vlsE*. Blood samples were taken prior to *Bb* infection (D0), at days 3 (D3) and 7 (D7) pi, and weekly thereafter including day 56 (D56). Raman spectra were collected from dried mouse blood samples. Most of vibrational bands in the acquired Raman spectra could be assigned to proteins and heme, with some likely belonging to other biomolecules (e.g., sugars and carotenoids), Figures 1, S9-S11, and Table 1. Although small changes were observed in the intensities of nearly all vibrational bands, the spectra collected from the preinfection blood (D0) were very similar to those of the postinfection samples (D3-D56). The overall results indicated that *Bb* infection-associated blood changes detectable by RS were very limited.

To determine whether Raman spectra could differentiate between various time points of *Bb* infection, PLS-DA was used. It was found that the prediction accuracy for binary differentiation of the spectra acquired from blood samples, which represented different time points of *Bb* infection, was predominantly high across the three *Bb* strains/mutant, Tables 2-4. The average TPR was 89% for B31 and Δ*vlsE*, and 86% for 297.

The lowest prediction accuracy was observed for B31 (53%) and 297 (64%) at D35. Additionally, it was found that the prediction accuracy for 297 at D3 and D42; D7 and D49; and D14 and D56 was lower compared to those identified for B31 and Δ*vlsE* at the respective time points. Together, this suggested that the biochemical profiles associated with mouse B31- or 297-induced infection at these time points were similar to those of healthy C3H mice. Overall, the results indicated that biochemical profiles of animal blood were changing as *Bb* infection progressed in C3H mice.

To determine which bands were *Bb* strain/mutant-specific, the unique spectra were assembled by taking the difference in the averages for each strain/mutant from each other at every time point, Figure S12. ANOVAs were conducted on the preprocessed spectra at band

TABLE 1 Vibrational band assignments for Raman spectra of mouse blood

Band (cm^{-1})	Assignment
562	Fe-O_2 stretch (heme)[59]
676	Pyrrole symmetric bending (Heme)[59]
719	C–C–O related to glycosidic ring skeletal deformations[60]
752	Protein,[61] Heme ring breathing[59]
962	Associated with alpha CH of porphyrin ring[62]
1002	Phenylalanine ring breathing[39], CH_3 in-plane rocking of polyenes[39]
1126	C–C stretching[39]
1172	Trp, Phe[61]
1226	CH Bending (Heme)[59]
1249	*meso* CH of porphyrin ring[62]
1275	Lipids, Amide III[61]
1308	*meso* CH of porphyrin ring[62]
1340	Trp, Adenine, Lipids[61]
1376	Pyrrole ring[63]
1447	CH_2[39]
1462	CH_2, CH_3[64]
1516	C=C[39]
1562	Conjugated CC stretching (heme)[59]
1579	C–C stretching[39]
1604	Aromatic ring[39]
1622	Aromatic ring[39]
1657	Amide I, C=C[39,50]
1681	Amide I,[64] carboxylic acids

TABLE 2 Prediction accuracy for *B. burgdorferi* 297

Day	0	3	7	14	21	28	35	42	49	56
0	n/a	1	0.785	0.92	0.935	0.86	0.64	0.98	0.77	0.97
3	1	n/a	0.89	0.9	0.91	0.91	0.895	0.67	0.895	0.845
7	0.785	0.89	n/a	0.985	0.81	0.91	0.765	0.935	0.655	0.955
14	0.92	0.9	0.985	n/a	0.91	0.905	0.9	0.915	0.805	0.68
21	0.935	0.91	0.81	0.91	n/a	0.89	0.84	0.885	0.875	0.875
28	0.86	0.91	0.91	0.905	0.89	n/a	0.77	0.865	0.785	0.855
35	0.64	0.895	0.765	0.9	0.84	0.77	n/a	0.9	0.735	0.91
42	0.98	0.67	0.935	0.915	0.885	0.865	0.9	n/a	0.87	0.85
49	0.77	0.895	0.655	0.805	0.875	0.785	0.735	0.87	n/a	0.925
56	0.97	0.845	0.955	0.68	0.875	0.855	0.91	0.85	0.925	n/a

TABLE 3 Prediction accuracy for *B. burgdorferi* B31

Day	0	3	7	14	21	28	35	42	49	56
0	n/a	0.867	0.902	0.91	0.9	0.835	0.535	0.92	0.97	1
3	0.867	n/a	1	0.84	0.83	0.91	0.885	0.91	0.945	1
7	0.902	1	n/a	0.9	0.725	0.92	0.93	0.98	0.955	1
14	0.91	0.84	0.9	n/a	0.9	0.845	0.875	0.855	0.91	0.94
21	0.9	0.83	0.725	0.9	n/a	0.94	0.905	0.935	0.96	0.985
28	0.835	0.91	0.92	0.845	0.94	n/a	0.82	0.91	0.91	0.99
35	0.535	0.885	0.93	0.875	0.905	0.82	n/a	0.9	0.92	0.965
42	0.92	0.91	0.98	0.855	0.935	0.91	0.9	n/a	0.8	0.867
49	0.97	0.945	0.955	0.91	0.96	0.91	0.92	0.8	n/a	0.765
56	1	1	1	0.94	0.985	0.99	0.965	0.867	0.765	n/a

TABLE 4 Prediction accuracy for the Δ*vlsE* mutant

Day	0	3	7	14	21	28	35	42	49	56
0	n/a	0.84	0.685	0.81	0.875	0.76	0.925	0.955	0.91	0.84
3	0.84	n/a	0.775	0.855	0.89	0.895	0.975	0.965	0.96	0.945
7	0.685	0.775	n/a	0.895	0.765	0.78	0.98	1	0.905	0.97
14	0.81	0.855	0.895	n/a	0.945	0.8375	0.975	0.92	0.85	0.86
21	0.875	0.89	0.765	0.945	n/a	0.88	0.985	0.98	0.965	1
28	0.76	0.895	0.78	0.8375	0.88	n/a	0.98	0.985	0.96	0.985
35	0.925	0.975	0.98	0.975	0.985	0.98	n/a	0.77	0.906	0.77
42	0.955	0.965	1	0.92	0.98	0.985	0.77	n/a	0.82	0.7475
49	0.91	0.96	0.905	0.85	0.965	0.96	0.906	0.82	n/a	0.8
56	0.84	0.945	0.97	0.86	1	0.985	0.77	0.7475	0.8	n/a

positions that appeared to vary across the *Bb* strains/mutant, Figures S1-S8.

Based on the ANOVA results (Table 5), no single band showed significant differences for all the time points. For example, at D56, 1251 and 1357 cm^{-1} (protein) and 1600 cm^{-1} (aromatic) could be used to differentiate between all three *Bb* strains/mutant. At D42, such confirmatory identification could be achieved by utilizing

TABLE 5 Summary of ANOVA results

Assigned Band	D7 Bands	D7 Groups	D14 Bands	D14 Groups	D21 Bands	D21 Groups	D28 Bands	D28 Groups	D35 Bands	D35 Groups	D42 Bands	D42 Groups	D49 Bands	D49 Groups	D56 Bands	D56 Groups
562	560	a-a-b			560	a-b-a			597	a-b-b						
719			710	ab-a-b												
752			764	a-b-b	745	a-a-b	739	a-a-b			738	a-ab-b	761	a-b-b	734	a-b-b
962															933	a-b-b
1002	1018	a-a-b							991	a-b-a						
1126							1126	a-b-ab								
1226					1217	a-b-a	1226	a-b-b	1231	a-b-a						
1249	1251	a-b-c	1251	a-b-c	1255	a-b-ab							1247	a-b-b	1251	a-b-c
1340	1358	a-b-a	1347	a-a-b					1341	a-b-a					1357	a-b-c
1376			1386	a-a-b	1371	ab-a-b	1377	a-a-b			1375	a-b-c	1362	a-b-b		
1447			1448	a-ab-b					1446	a-b-c	1456	a-b-a				
1516			1524	a-b-b	1516	a-b-a	1527	a-b-a	1494	a-b-a			1533	a-b-b	1525	a-b-b
1562	1567	a-b-a			1551	a-b-ab	1556	a-b-b	1551	a-b-c	1549	a-b-c				
1604			1591	a-ab-b					1610	a-b-c	1600	a-b-b	1606	a-b-b	1600	a-b-c
1622	1632	a-b-a			1627	a-b-b					1627	a-b-c				
1657							1646	a-b-b							1647	a-a-b

Note: The letter order of groups is 297-Δ*vlsE*-B31. The letters indicate significantly different groups. Two letters indicate that the group in question is not significantly different from either of the other two groups. Figures S1-S8 provide 95% confidence intervals for the true mean intensity of bands for *B. burgdorferi* 297, B31, and ΔvlsE at day 7 postinfection.

1357 cm^{-1} (protein) and 1627 cm^{-1} (aromatic) vibrations. From the reported ANOVAs, the most frequently occurring bands, 752 and 1516 cm^{-1}, were identified for 6 of the 8 time points (Figures S1-S8). These two bands could be assigned to heme ring breathing and carbon-carbon double-bonds. Also, statistically significant differences were observed for only some time points and only between some strain/mutant comparisons. For example, D14 blood of 297-infected mice was significantly different from that of B31- or Δ*vlsE*-infected mice. In contrast, for D21 blood samples, the significant difference was detected between the Δ*vlsE*-infected mice and 297- or B31-infected animals (Figures S2 and S3). The latter may be partially explained by the fact that, as opposed to the wild-type *Bb* strains, the Δ*vlsE* mutant is consistently cleared by an anti-*Bb* immune response of C3H mice by D21 due to its lack of VlsE antigenic variation system.[43,49]

4 | DISCUSSION

The present study has investigated whether RS had the capacity to detect *Bb* infection in C3H mice. The data demonstrated that RS had a limited resolution in identification of blood metabolites associated with *Bb* infection of mice at the molecular species level. For some RS-detectable vibrational bands, this limitation seemed to be unavoidable. For example, all proteins had a vibrational band around 1657 cm^{-1} (amide I), which originates from the peptide bond vibration.[34] At the same time, this vibration could be also derived from alkene groups of unsaturated fatty acids.[50] Despite, however, its failure to define the molecular species, whose blood levels would change over *Bb* infection, RS was still very sensitive at detecting subtle changes in the blood biochemistry profiles of infected mice. The overall data showed that biochemical changes in blood of *Bb*-infected C3H mice was consistently detected (and often with high accuracy) as early as at D3 pi and at much later time points of mouse infection (e.g., D49, D56).[45,51]

The current investigation has also examined whether identification of *Bb*-induced infection was directly dependent on the presence of *Bb* spirochetes in mouse blood. The obtained experimental evidence strongly indicated that this detection was not direct. First, vibrational bands that could be assigned to *Bb* spirochetal components were not identified in blood samples taken at any of the time points, including D7 at which culture-detectable spirochetemia is consistently high.[45,51] Second, RS allowed B31- or 297-infected mice to be equally detected both at the early stage of *Bb* infection (e.g., D3, D7), when *Bb* was present in mouse blood; and later time points (e.g., D21, D56), when spirochetes had already left the blood and resided in other mouse tissues (e.g., bladder, joints, heart) that often serve as protective niches for *Bb*.[45,51,52] Lastly, RS consistently detected metabolic changes in blood of Δ*vlsE*-infected mice from D21 through D56, the time period, when live Δ*vlsE* spirochetes were no longer present in the mice due to their antibody-mediated clearance.[43,53–57]

Despite the failure of RS to directly detect *Bb* spirochetes in mouse blood, the average TPR was equally high for all the strains/mutant tested, 89% for B31 and Δ*vlsE*, and 86% for 297. Moreover, the data also suggested that pathogen-induced changes in the host metabolism were *Bb* strain-specific. To prove the latter, however, future research involving much more *Bb* strains as well as other *Borreliella* genospecies are needed.

Finally, despite a limited number of samples analyzed, the overall results of this proof-of-concept study are encouraging and warrant further exploration of RS diagnostic utility for LD. Future investigation should be expanded by including much more mouse blood samples and also diagnostic specimens from human LD patients. To obtain the latter, the Lyme Disease Biobank (LDB), which is the unique biorepository of blood samples collected from clinically characterized patients with and without LD, could be conveniently used.[58] Further study should also address the specificity of LD-associated spectra in regard to other human (tick-borne) infectious agents, the critical question that will require a long-term and well-funded investigation.

ACKNOWLEDGMENTS

The authors would like to thank Ms. Maliha Batool for technical assistance with blood sample collection. The study was supported by the Bay Area Lyme Foundation via the Emerging Leader Award.

DATA AVAILABILITY STATEMENT

Research data are not shared.

ORCID

Dmitry Kurouski https://orcid.org/0000-0002-6040-4213
Artem S. Rogovskyy https://orcid.org/0000-0001-6499-7928

REFERENCES

[1] A. F. Hinckley, N. P. Connally, J. I. Meek, B. J. Johnson, M. M. Kemperman, K. A. Feldman, J. L. White, P. S. Mead *Clin. Infect. Dis.* **2014**, *59*, 676–681.
[2] D. J. Cameron, L. B. Johnson, E. L. Maloney *Expert Rev. Anti. Infect. Ther.* **2014**, *12*, 1103–1135.
[3] B. J. Hudson, M. Stewart, V. A. Lennox, M. Fukunaga, M. Yabuki, H. Macorison, J. Kitchener-Smith *Med. J. Aust.* **1998**, *168*, 500–502.

[4] J. Oksi, M. Marjamaki, J. Nikoskelainen, M. K. Viljanen *Ann. Med*. **1999**, *31*, 225–232.

[5] N. Kash, R. Fink-Puches, L. Cerroni *Am. J. Dermatopathol.* **2011**, *33*, 712–715.

[6] M. J. Middelveen, E. Sapi, J. Burke, K. R. Filush, A. Franco, M. C. Fesler, R. B. Stricker *Healthcare (Basel).* **2018**, *6*.

[7] E. L. Logigian, R. F. Kaplan, A. C. Steere *N. Engl. J. Med.* **1990**, *323*, 1438–1444.

[8] G. Stanek, J. Klein, R. Bittner, D. Glogar *N. Engl. J. Med.* **1990**, *322*, 249–252.

[9] A. Vaz, L. Glickstein, J. A. Field, G. McHugh, V. K. Sikand, N. Damle, A. C. Steere *Inf. Immun.* **2001**, *69*, 7437–7444.

[10] T. J. LaRocca, J. L. Benach *Curr. Top. Microbiol. Immunol*. **2008**, *319*, 63–103.

[11] Y. Xu, J. F. Bruno, B. J. Luft *Microb. Pathogen*. **2008**, *45*, 403–407.

[12] M. B. Lawrenz, J. M. Hardham, R. T. Owens, J. Nowakowski, A. C. Steere, G. P. Wormser, S. J. Norris *J. Clin. Microbiol.* **1999**, *37*, 3997–4004.

[13] S. L. Arvikar, A. C. Steere *Infect. Dis. Clin. North. Am*. **2015**, *29*, 269–280.

[14] P. M. Lantos *Infect. Dis. Clin. North. Am.*. **2015**, *29*, 325–340.

[15] M. T. Melia, P. M. Lantos, P. G. Auwaerter *J.Am. Ass. Neurol.* **2015**, *72*, 126.

[16] A. T. Borchers, C. L. Keen, A. C. Huntley, M. E. Gershwin *J. Authoimmun.* **2015**, *57*, 82–115.

[17] A. R. Marques *Curr. Allergy Asthma. Rep.* **2010**, *10*, 13–20.

[18] G. P. Wormser, R. J. Dattwyler, E. D. Shapiro, J. J. Halperin, A. C. Steere, M. S. Klempner, P. J. Krause, J. S. Bakken, F. Strle, G. Stanek, L. Bockenstedt, D. Fish, J. S. Dumler, R. B. Nadelman *Clin. Infect. Dis*. **2006**, *43*, 1089–1134.

[19] L. R. Lindsay, K. Bernat, A. Dibernardo *Can. Commun. Dis. Rep.* **2014**, *40*, 209–217.

[20] L. A. Waddell, J. Greig, M. Mascarenhas, S. Harding, R. Lindsay, N. Ogden *PLoS One.* **2016**, *11*.

[21] C. Centers for Disease, Prevention *M. M. W. R. Morb. Mortal. Wkly. Rep*. **1995**, *44*, 590–591.

[22] E. Hilton, J. DeVoti, J. L. Benach, M. L. Halluska, D. J. White, H. Paxton, J. S. Dumler *Am. J. Med*. **1999**, *106*, 404–409.

[23] R. M. Bacon, B. J. Biggerstaff, M. E. Schriefer, R. D. Gilmore, Jr., M. T. Philipp, A. C. Steere, G. P. Wormser, A. R. Marques, B. J. Johnson *J. Inf. Dis*. **2003**, *187*, 1187–1199.

[24] M. E. Aguero-Rosenfeld, G. Wang, I. Schwartz, G. P. Wormser *Clin. Microbiol. Rev.* **2005**, *18*, 484–509.

[25] M. Lager, R. B. Dessau, P. Wilhelmsson, D. Nyman, G. F. Jensen, A. Matussek, P. E. Lindgren, A. J. Henningsson, G. ScandTick Biobank Study, H. Baqir, L. Serrander, M. Johansson, I. Tjernberg, I. Skarstein, E. Ulvestad, N. Grude, A. B. Pedersen, A. Bredberg, R. Veflingstad, L. Wass, J. Aleke, M. Nordberg, C. Nyberg, L. Perander, C. Bojesson, E. Sjoberg, A. R. Lorentzen, R. Eikeland, S. Noraas, G. A. Henriksson, G. Petranyi *Eur. J. Clin. Microbiol. Infect. Dis.* **2019**, *38*, 1933–1945.

[26] S. E. Schutzer, B. A. Body, J. Boyle, B. M. Branson, R. J. Dattwyler, E. Fikrig, N. J. Gerald, M. Gomes-Solecki, M. Kintrup, M. Ledizet, A. E. Levin, M. Lewinski, L. A. Liotta, A. Marques, P. S. Mead, E. F. Mongodin, S. Pillai, P. Rao, W. H. Robinson, K. M. Roth, M. E. Schriefer, T. Slezak, J. L. Snyder, A. C. Steere, J. Witkowski, S. J. Wong, J. A. Branda *Clin. Infect. Dis*. **2019**, *68*, 1052–1057.

[27] P. Coulter, C. Lema, D. Flayhart, A. S. Linhardt, J. N. Aucott, P. G. Auwaerter, J. S. Dumler *J. Clin. Microbiol.* **2005**, *43*, 5080–5084.

[28] M. S. Klempner, C. H. Schmid, L. Hu, A. C. Steere, G. Johnson, McCloud, B., R. Noring, A. Weinstein *Am. J. Med.* **2001**, *110*, 217–219.

[29] S. H. Lee, J. S. Vigliotti, V. S. Vigliotti, W. Jones, D. M. Shearer *Int. J. Mol. Sci.* **2014**, *15*, 4284–4298.

[30] A. Moore, C. Nelson, C. Molins, P. Mead, M. Schriefer *Emerg. Inf. Dis.*. **2016**, 22.

[31] W. Liu, H. X. Liu, L. Zhang, X. X. Hou, K. L. Wan, Q. Hao *Int. J. Mol. Sci.* **2016**, 17.

[32] O. Nolte *Open Neurol. J.* **2012**, *6*, 129–139.

[33] I. Bil-Lula, P. Matuszek, T. Pfeiffer, M. Wozniak *Adv. Clin. Exp. Med.* **2015**, *24*, 663–670.

[34] D. Kurouski, R. P. van Duyne, I. K. Lednev *Analyst.* **2015**, *140*, 4967–4980.

[35] N. M. Ralbovsky, I. K. Lednev *Chem. Soc. Rev.* **2020**, *49*, 7428–7453.

[36] C. S. Ho, N. Jean, C. A. Hogan, L. Blackmon, S. S. Jeffrey, M. Holodniy, N. Banaei, A. A. E. Saleh, S. Ermon, J. Dionne *Nat. Commun.* **2019**, *10*, 4927.

[37] E. Ryzhikova, O. Kazakov, L. Halamkova, D. Celmins, P. Malone, E. Molho, E. A. Zimmerman, I. K. Lednev *J. Biophotonics.* **2015**, *8*, 584–596.

[38] A. J. Hobro, A. Konishi, C. Coban, N. I. Smith *Analyst.* **2013**, *138*, 3927–3933.

[39] S. Khan, R. Ullah, M. Saleem, M. Bilal, R. Rashid, I. Khan, A. Mahmood, M. Nawaz *Optik.* **2016**, *127*, 2086–2088.

[40] C. R. Molins, L. V. Ashton, G. P. Wormser, A. M. Hess, M. J. Delorey, S. Mahapatra, M. E. Schriefer, J. T. Belisle *Clin. Infect. Dis.* **2015**, *60*, 1767–1775.

[41] A. F. Elias, P. E. Stewart, D. Grimm, M. J. Caimano, C. H. Eggers, K. Tilly, J. L. Bono, D. R. Akins, J. D. Radolf, T. G. Schwan, P. Rosa *Inf. Immun.* **2002**, *70*, 2139–2150.

[42] C. A. N. Hughes, C. B. Kodner, R. C. Johnson *J. Clin. Microbiol.* **1992**, *30*, 698–703.

[43] T. Bankhead, G. Chaconas. *Mol. Microbiol.* **2007**, *65*, 1547–1558.

[44] A. S. Rogovskyy, D. C. Gillis, Y. Ionov, E. Gerasimov, A. Zelikovsky *Inf. Immun...* **2017**, 85.

[45] S. W. Barthold, D. S. Beck, G. M. Hansen, G. A. Terwilliger, K. D. Moody *J. Inf. Dis.* **1990**, *162*, 133–138.

[46] D. Liveris, S. Varde, R. Iyer, S. Koenig, S. Bittker, D. Cooper, D. McKenna, J. Nowakowski, R. B. Nadelman, G. P. Wormser, I. Schwartz *J. Clin. Microbiol.* **1999**, *37*, 565–569.

[47] D. Liveris, G. P. Wormser, J. Nowakowski, R. Nadelman, S. Bittker, D. Cooper, S. Varde, F. H. Moy, G. Forseter, C. S. Pavia, I. Schwartz *J. Clin. Microbiol.* **1996**, *34*, 1306–1309.

[48] A. S. Rogovskyy, T. Casselli, Y. Tourand, C. R. Jones, J. P. Owen, K. L. Mason, G. A. Scoles, T. Bankhead *PLoS One.* **2015**, *10*, e0124268.

[49] A. S. Rogovskyy, T. Bankhead *PLoS One.* **2013**, *8*, e61226.

[50] C. Farber, L. Sanchez, S. Rizevsky, A. Ermolenkov, B. McCutchen, J. Cason, C. Simpson, M. Burrow, D. Kurouski *Sci. Rep.* **2020**, *10*, 7730.

[51] S. Barthold, D. Persing, A. Armstrong, R. Peeples *Am. J. Pathol.* **1991**, *139*, 263–273.
[52] F. T. Liang, E. L. Brown, T. Wang, R. V. Iozzo, E. Fikrig *Am. J. Pathol.* **2004**, *165*, 977–985.
[53] J. E. Purser, S. J. Norris *Proc. Nat. Acad. Sci. U. S. A.* **2000**, *97*, 13865–13870.
[54] M. Labandeira-Rey, J. T. Skare *Inf. Immun.* **2001**, *69*, 446–455.
[55] M. Labandeira-Rey, J. Seshu, J. T. Skare *Inf. Immun.* **2003**, *71*, 4608–4613.
[56] R. Iyer, O. Kalu, J. Purser, S. Norris, B. Stevenson, I. Schwartz *Inf. Immun.* **2003**, *71*, 3699–3706.
[57] M. B. Lawrenz, R. M. Wooten, S. J. Norris *Inf. Immun.* **2004**, *72*, 6577–6585.
[58] E. J. Horn, G. Dempsey, A. M. Schotthoefer, U. L. Prisco, M. McArdle, S. S. Gervasi, M. Golightly, C. de Luca, M. Evans, B. S. Pritt, E. S. Theel, R. Iyer, D. Liveris, G. Wang, D. Goldstein, I. Schwartz *J. Clin. Microbiol.* **2020**, *58*.
[59] M. Casella, A. Lucotti, M. Tommasini, M. Bedoni, E. Forvi, F. Gramatica, G. Zerbi *Spectrochim. Acta A Molecul. Biomol. Spectrosc.* **2011**, *79*, 915–919.
[60] M. Krimmer, C. Farber, D. Kurouski *ACS Omega.* **2019**, *4*, 16330–16335.
[61] J. L. Pichardo-Molina, C. Frausto-Reyes, O. Barbosa-García, R. Huerta-Franco, J. L. González-Trujillo, C. A. Ramírez-Alvarado, G. Gutiérrez-Juárez, C. Medina-Gutiérrez. *Laser. Med. Sci.* **2007**, *22*, 229–236.
[62] P. Lemler, W. R. Premasiri, A. DelMonaco, L. D. Ziegler Anal. *Anal. Bioanal.* **2014**, *406*, 193–200.
[63] C. G. Atkins, K. Buckley, M. W. Blades, R. F. B. Turner. *Appl. Spectrosc.* **2017**, *71*, 767–793.
[64] G. Başar, U. Parlatan, Ş. Şeninak, T. Günel, A. Benian, İ. Kalelioğlu. *J. Spectrosc.* **2012**, *27*, 239–252.

SUPPORTING INFORMATION

Additional supporting information may be found online in the Supporting Information section at the end of this article.

How to cite this article: Farber C, Morey R, Krimmer M, Kurouski D, Rogovskyy AS. Exploring a possibility of using Raman spectroscopy for detection of Lyme disease. *J. Biophotonics*. 2021; e202000477. https://doi.org/10.1002/jbio.202000477